Current Colorectal Cancer Reports (2021) 17:77–87
https://doi.org/10.1007/s11888-021-00470-x

RADIATION THERAPY AND RADIATION THERAPY INNOVATIONS IN COLORECTAL CANCER (P LEE AND A RALDOW, SECTION EDITORS)

Recent Advances in Functional MRI to Predict Treatment Response for Locally Advanced Rectal Cancer

Yu Gao[1] · Jonathan Pham[1,2] · Stephanie Yoon[1] · Minsong Cao[1,2] · Peng Hu[2,3] · Yingli Yang[1,2]

Accepted: 19 August 2021 / Published online: 12 November 2021

Abstract

Purpose of Review Early response prediction for locally advanced rectal cancer (LARC) provides an opportunity for response-tailored treatment management. The goal of this review is to summarize recent advances in applying functional MRI, such as diffusion-weighted imaging (DWI) and dynamic contrast-enhanced MRI (DCE-MRI), to predict treatment response for LARC patients, as well as to discuss the associated limitations and future directions.

Recent Findings Many recent studies incorporated advanced data analysis methods, such as radiomics and deep learning, to enhance prediction performance. Multi-parametric imaging has also become a trend that utilizes complementary information from each technique. However, there are wide variations in patient enrollment, imaging time points, scan parameters, and treatment response endpoint definitions, which leads to a range of findings among these studies. Moreover, small sample size and lack of independent validation of most studies also weaken conclusions.

Summary Functional MRI has been shown as a potential early biomarker for rectal cancer treatment response estimation. To incorporate functional MRI into clinical workflow, future work with large standardized data are warranted.

Keywords Rectal cancer · Functional MRI · Treatment response · DWI · DCE

Introduction

Neoadjuvant therapy is standard of care for patients with locally advanced rectal adenocarcinomas. These patients have primary tumors that either extend beyond the muscularis propria and into the surrounding subserosa, abut or are fixed to nearby structures (including the pelvic sidewalls, bladder, rectum, and sacrum), or tumors that have metastasized to draining pelvic lymph nodes. Long-course chemoradiation (LCRT) has traditionally been employed in the neoadjuvant setting. This involves concurrent delivery of 5-fluorouracil (5-FU) with radiation delivered in 28 fractions to a total dose of 50.4 Gy followed by total mesorectal excision (TME) 6–8 weeks later [1–3].

The French FFCD9203 and German Rectal Cancer Trials demonstrated that the best local tumor control can be achieved with neoadjuvant LCRT [1, 2]. The French FFCD9203 trial showed a significantly lower 5-year local recurrence rate with neoadjuvant chemoradiation compared to radiation therapy alone [1]. In the German Rectal Cancer Trials, patients receiving neoadjuvant chemoradiation experienced significantly fewer local relapses compared to adjuvant chemoradiation [2]. However, both trials did not shown reduction in distant metastatic failure or improvements in overall survival with neoadjuvant LCRT. In fact, most rectal cancer patients fail at distant sites (~30% of the time), and 5-year overall survival from advanced rectal cancer remains is 65–75% [4–6].

Attempts to improve clinical outcomes from traditional neoadjuvant regimens have led to several areas of investigation. One such area is to identify subsets of patients who

Yu Gao and Jonathan Pham contributed equally to this work

This article is part of the Topical Collection on *Radiation Therapy and Radiation Therapy Innovations in Colorectal Cancer*

✉ Yingli Yang
yyang@mednet.ucla.edu

[1] Department of Radiation Oncology, University of California, Los Angeles, 200 UCLA Medical Plaza Suite B265, Los Angeles, CA 90095, USA

[2] Physics and Biology in Medicine IDP, University of California, Los Angeles, 200 UCLA Medical Plaza Suite B265, Los Angeles, CA 90095, USA

[3] Department of Radiological Sciences, University of California, Los Angeles, Los Angeles, CA, USA

would be good or poor treatment responders early in their treatment course to tailor their subsequent management of the disease. Assessment of rectal cancer treatment response is mainly based on histopathology evaluation using different tumor regression grade (TRG) such as Dworak's grading system, Ryan grading system, or Mandard grading system [7–9]. Pathological complete response (pCR) is defined as absence of viable tumor cells in the surgical specimen. Good response (GR) usually refers to complete or near-complete regression, while the remaining is non-respective (non-GR).

Early treatment response prediction provides a window for treatment adaptation and opens the door to personalized treatment. With traditional treatment paradigms, 10–30% of patients had a complete pathological response [10–12]. Whether surgery can be avoided in these responders to reduce surgical complications and to improve their long-term quality of life becomes an active area of research [13–15]. A reliable early tumor response assessment mechanism is essential to guide patient-tailored treatments. Functional MRI, such as diffusion-weighted MRI (DWI) and dynamic contrast-enhanced MRI (DCE-MRI), has long been used for treatment response prediction for rectal cancer patients [16–19]. They provide a noninvasive measurement of tumor functional information such as cellularity and vascularization. This information could potentially detect treatment response before tumor size change [20, 21], which is used in the RECIST criteria [22].

There have been several review papers summarizing applications of functional MRI for treatment response prediction in rectal cancer [16–19]. In this review, we focused on summarizing recent literature, more specifically articles published after 2017, to bring the reader up-to-date on the current advances of using functional MRI, in particular DWI and DCE, for rectal tumor treatment response assessment.

Functional MRI

Diffusion-Weighted MRI

Diffusion-weighted MRI is one of the most widely used functional MRI techniques for tumor response assessment. It quantifies the random Brownian motion of water molecules at the voxel level, and provides tissue morphofunctional information including cellular density. In DWI imaging, the detected signal level S_b decreases exponentially with tissue intrinsic diffusivity D and the b-value: $S_b/S_0 = \exp(-bD)$, where the b-value is determined by the pulse gradient waveform, and S_0 is the signal intensity at $b = 0$ s/mm^2. Therefore, by applying at least two different b-values, the derived parameter apparent diffusion coefficient (ADC) reflects tissue cellularity information. Because of its ability to reflect tissue functional information, DWI has been used alone or in combination with other imaging, such as T2-weighted imaging (T2w), for response assessment.

Studies have shown that incorporating DWI into tumor regression grading may improve interobserver agreement and provide better agreement with the pathological response or disease-free survival (DFS) prediction for patients with LARC having undergone neoadjuvant chemoradiotherapy (CRT) [23–25]. Heeswijk et al. and Gollub et al. showed that despite false-positive findings, the absence of node on DWI images is a reliable predictor of yN0, and tumor-bed diffusion restriction from DWI detects tumor recurrence before endoscopy [26, 27]. Shaverdian et al. acquired longitudinal DWI (every 3–7 days) on a low-field MR-guided radiotherapy system on three patients. They found the trend of ADC changes correlated with pathological response [28].

In addition to being used as a qualitative assessment tool, DWI has also been used extensively as a quantitative predictor of treatment response (Table 1) [29–35]. However, due to heterogeneity of patient enrollment, patient cohort size, image acquisition, data processing, and analysis methods, there is a range of findings among these studies. For example, De Felice et al. acquired DWI prior, during, and post-CRT on 37 patients, and found the mid-CRT ADC value significantly increased in the pCR group [29], whereas in a similar study, median pre-CRT ADC was more predictive of pathological response [30]. Moreover, several other researchers found that the mean post-CRT ADC value is most predictive of differentiating pCR [31, 32]. In another study, Tarallo et al. analyzed pre- and post-CRT MRIs on 32 LARC patients and concluded that both ADC and ADC change were not reliable predictors of CR, and post-CRT tumor volume based on DWI and tumor volume change were more accurate in discriminating CR from non-CR [33]. Crimi et al. also did not find a significant correlation between ADC and tumor complete regression based on their prospective study with 22 patients [34]. Bulens et al. built a multivariate model using two T2-volumetric and two DWI parameters from pre- and post-CRT MRI, and achieved 0.88 area under the ROC curve (AUC) in an external validation cohort [35]. Both Joye et al. and Schurink et al. showed that PET/CT was worse than MRI in rectal cancer response assessment [36, 37], indicating the functional information provided by MRI is more predictive than molecular markers from PET/CT. However, the latter group concluded that pre-treatment DWI was inferior to T2w MRI. Given the wide variation of findings, imaging acquisition standardization and external validation are urgently needed.

In the last few decades, more advanced prediction models such as radiomics and deep learning have been applied in rectal cancer treatment response assessment [38••, 39–44]. By extracting high-dimensional quantitative features, it aims to uncover predictive information that is not obvious to human eyes [45]. Some of the key findings of

Table 1 Summary of some key quantitative studies of using DWI for response assessment

Study	*n*	Study design	Imaging	Treatment response	Key results
De Felice et al. (2017) [29]	37	Prospective	Pre-, mid-, post-CRT 3 T DWI and T2w MRI	pCR (ypT0 ypN0) No-pCR (other)	Mid-CRT mean ADC significantly increased in the pCR group. No substantial difference in the ADC distribution was found pCR and no-pCR patients
Palmisano et al. (2020) [30]	43	Prospective	Pre-, mid-, post-CRT 1.5 T DWI and T2w MRI	Rodel TRG Non-responders (TRG0-2) Partial responder (TRG3) Complete responders (TRG4)	Median pre-CRT ADC and ΔVb,1,000 (from pre-to-post-CRT) are good predictors of CR (accuracy of 86% and 86.8%)
Yang et al. (2019) [31]	76	Retrospective	Post-CRT 3 T DWI and T2w MRI	TRG Responder (TRG0) Non-responder (TRG1-3)	Mean post-CRT ADC was significantly higher in pCR group. ROC AUC value was 0.912
Tarallo et al. (2018) [33]	32	Retrospective	Pre- and post-CRT 1.5 T DWI and T2w MRI	Dworak TRG Responder (TRG4) Non-responder (TRG1-3)	Post-CRT VDWI and ΔVDWI% have perfect AUC of 1 for CR assessment. ADC and ΔADC% values, on the contrary, are not reliable predictors (AUC < 0.6)
Bulens et al. (2018) [35]	140	Prospective	Pre- and post-CRT 3 T DWI and T2w MRI	Near-complete response: ypT0-1N0 Non-responder: the remaining	A multivariate model using two T2-volumetric and two DWI parameters achieved AUC of 0.88 in an external cohort
Schurink et al. (2020) [37]	61	Retrospective	Pre-CRT PET/CT, 1.5 T DWI and T2w MRI	Mandard TRG GR: TRG1-2 Non-GR: TRG3-5	The multivariable model incorporating mrT-stage and quantitative features from T2w-MRI achieved AUC of 0.83. Pre-treatment PET/CT or DWI did not contribute to the predictive performance
Joye et al. (2017) [36]	85	Prospective	Pre-, mid-, and post-CRT PET/CT, 3 T DWI and T2w MRI	Responder: ypT0-1N0 Non-responder: others	PET/CT had worse predictive performance than DWI and T2 (0.61 vs. 0.72 vs. 0.72). Combining all features increased AUC to 0.81
Tang et al. (2019) [38••]	222	Retrospective	Pre- and post-CRT 3 T DWI and T2w MRI	pGR (down-staging to ypT0-1N0) Non-pGR (others)	Prediction model with clinical information alone had AUC of 0.631. DWI radiomics provided AUC of 0.866. Combination of DWI radiomics and clinical characteristics improved AUC to 0.890
Bulens et al. (2020) [39]	125	Prospective	Pre- and post-CRT 3 T DWI and T2w MRI	pCR: ypT0–1N0 Non-pCR: others	Two models with t2_dwi_pre_post, semantic_dwi_post had ≥ 0.83 AUC on both training and external validation cohort
Chen et al. (2020) [40]	80	Retrospective	3 T DWI, T2w, and T1VIBE MRI	Local recurrence confirmed by colonoscopy biopsy (at least 24-mo follow-up)	Radiomics model combining features from DWI, T2w, and T1VBE provided 0.864 AUC on the validation set
Wan et al. (2020) [41]	165	Retrospective	Pre- and post-CRT 3 T DWI and T2w MRI	pCR(ypT0N0) Non-pCR: others	Combined model with T2WI and DWI delta-radiomics signature had 0.91 AUC on both training and testing cohort. This was much better than visual assessment by expert radiologist

those studies are summarized in Table 1. Griethuysen et al. compared response prediction between expert radiologists' visual morphologic assessment and radiomics models using staging MRIs on 133 patients, and found comparable results between the two methods in predicting pCR and GR [42]. In a large study with 222 patients, Tang et al. combined pre-CRT and pre-surgery DWI radiomics features with clinical characteristics, and the combined model provided an AUC of 0.89 in identifying pathological good response of down-staging to ypT0-1N0 on the independent validation set [38••]. By visual comparison, they showed that one radiomics feature, Neighborhood Gray Tone Difference Matrix (TGTDM), appeared brighter after CRT for the pGR patient, whereas the contrast remained unchanged for the non-pGR patient (Fig. 1). Bulens et al. extracted radiomics and semantic features from T2w, DWI, and ADC images acquired before and after CRT. After principal component analysis (PCA) and LASSO regression analysis, the optimal model provided a 0.86 AUC of pGR prediction on an external cohort [39]. Chen et al. found that by adding T2w and contrast-enhanced T1-weighted volume interpolated body examination (VIBE) in addition to DWI radiomics, the model AUC increased from 0.75 to 0.86 [40]. In a retrospective study with 165 LARC patients, Wan et al. found that delta-radiomics, defined as percentage change of a radiomics feature from pre- to post-CRT MRI, had the highest AUC [41]. Nardone et al. showed that radiomics features from pre-CRT DWI may be helpful in identifying patients that develop early progression [43]. To compare prediction performance using radiomics features with deep learning-based (DL) features, Fu et al. compared the LASSO-logistic regression models using radiomics and DL-based features based on pre-CRT DWIs on 43 patients. They found DL-based features significantly outperformed radiomics features (AUC 0.73 v.s. 0.64) [44].

The conventional DWI assumes mono-exponential signal decay with respect to the *b*-value. However, Le Bihan et al. found that at lower *b*-values, especially less than 200 s/mm^2, the signal attenuation is primarily due to microcirculation of blood in the capillary network, or microscopic perfusion [46]. The proposed intravoxel incoherent motion (IVIM) model formulates signal decay as the following:

$$S_b/S_0 = (1-f)exp(-bD) + fexp(-bD^*)$$

where f is the perfusion fraction, D is the true diffusion coefficient, and D^* is the pseudo-diffusion coefficient. To estimate IVIM parameters, a series of DWI images including several low *b*-value images were acquired. Several studies found that IVIM-derived D value or $\Delta\%D$ provided higher performance than the conventional ADC value [47–49] in terms of response prediction. Zhu et al. and Liang et al. applied the stretched-exponential model (SEM) to derive the distributed diffusion coefficient (DDC) and heterogeneity index α. Both groups claim that ADC and SEM-derived parameters were superior to IVIM models in pCR

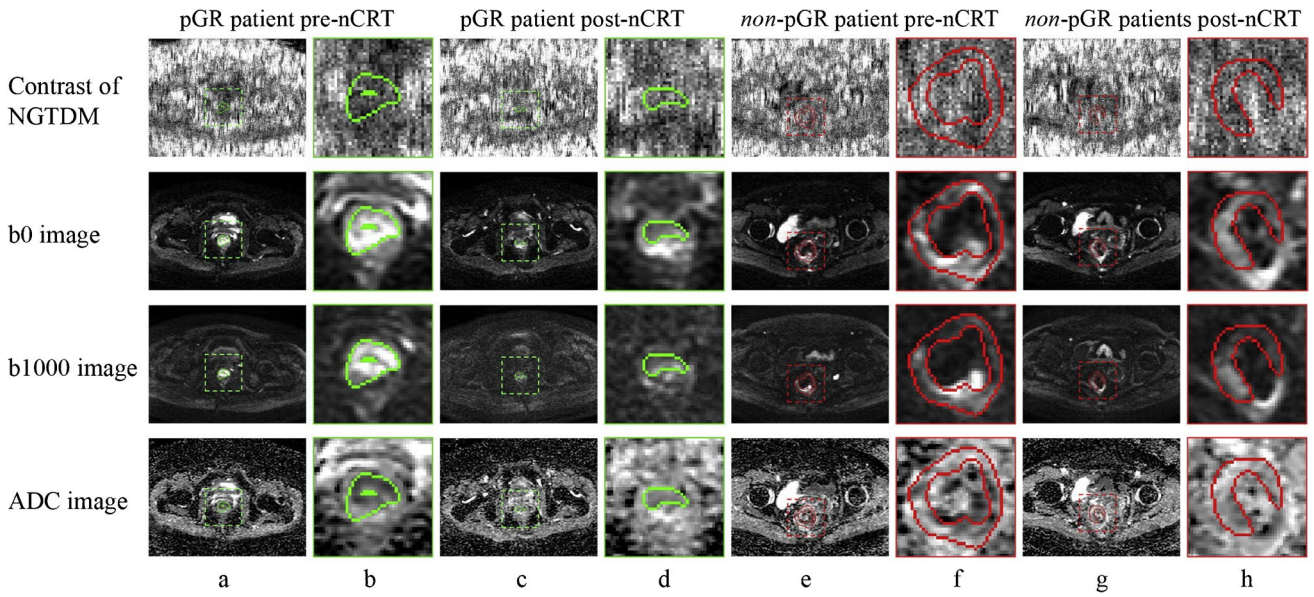

Fig. 1 The voxel-based contrast of NGTDM and original MR images of pGR and non-pGR patients. The voxel-based contrast of NGTDM, *b*0, *b*1000, and ADC images of pGR and non-pGR patients is displayed in each row. Columns (a) and (c) represent the pre- and post-nCRT images of the pGR patient. Columns (b) and (d) are the enlarged tumor regions in (a) and (c). Columns (e) and (g) represent the pre- and post-nCRT images of the non-pGR patient. Columns (f) and (h) are the corresponding enlarged tumor regions in (e) and (g). Image from Tang et al. [38••]. Reprinted with permission

prediction [50, 51]. To evaluate IVIM texture features for pCR assessment, Liu et al. acquired IVIM-DWI prospectively on 41 patients 1–3 days before CRT. They found that IVIM-derived parameters and first-order texture features did not show statistically significant differences between pCR and non-pCR. Several higher-order texture features had significant differences between the two groups, and the highest AUC was 0.837 [52]. One issue with those studies is that IVIM protocols were not uniform across the studies. A total of 9 to 16 *b*-values were applied in the acquisition, with the maximum *b* value between 800 and 2000s/mm^2.

DWI also assumes water diffusion within a voxel follows a Gaussian behavior. However, non-Gaussian behavior becomes more obvious at higher *b*-values and this leads to a lower than expected apparent diffusion coefficient. This non-Gaussian diffusion kurtosis imaging (DKI) proposes the signal decay as $S_b/S_0 = \exp(-bD + 16b^2D^2k)$, where k is the diffusion kurtosis coefficient that reflects molecular motion deviation from Gaussian distribution [53]. In one prospective study with 56 patients, pre- and post- CRT MRI were acquired, and ADC, mean diffusion (MD), mean kurtosis (MK), and their change ratios before and after CRT were calculated. They found that DKI was overall better than ADC in differentiating pCR from non-pCR, and MKpost was found to be the most promising parameters [54].

Dynamic Contrast-Enhanced MRI

DCE-MRI uses a series of MRIs to measure the T1 change of an injected contrast agent, usually gadolinium (Gd), between the vasculature and interstitial space. T1-weighted 3D-spoiled gradient echo technique is usually used for imaging. After imaging, the DCE intensity is converted to gadolinium concentration for concentration–time curve analysis. DCE provides information on tissue vascularization, perfusion, capillary permeability, and composition of the interstitial space. Malignant and aggressive neoplasms tend to have a greater degree of vascularity to supply nutrients to the rapidly proliferating cells. As a result, DCE has been theorized to be a promising diagnostic and treatment response tool for rectal cancer patients undergoing CRT.

DCE-MRI's concentration–time curves can be evaluated visually, semi-quantitatively, or quantitatively. The key findings in DCE studies for CRT treatment response are shown in Table 2. In visual DCE analysis, patterns of contrast uptake are observed, and tissue blood flow, blood volume, capillary area/permeability, and tissue extracellular space are qualitatively evaluated. In a visual DCE study with 158 LARC patients, Petrillo et al. showed that visually inspecting DCE after CRT was superior to morphological MRI using T2-weighted MRI for predicting CRT responders [55]. DCE achieved sensitivity, specificity, and the accuracy of 81%, 85%, and 82%, while T2-weighted MRI achieved 52%, 78%, and 62%, respectfully.

In semi-quantitative DCE analysis, DCE concentration–time curve's peak, slope (wash-in/out rate), and AUC are measured. In a prospective semi-quantitative DCE study with 28 LARC patients, Ippolito et al. showed perfusion was significantly higher in rectal cancer tumor tissue than in healthy tissue. Moreover, prior to CRT, there was no significant difference in perfusion parameters between responders and non-responders, whereas after CRT, responders showed significantly lower perfusion values than non-responders. Additionally, responder perfusion values decreased significantly from pre- to post-cRT [56]. In contrast, Attenberger et al. showed the change in perfusion, after CRT, did not correlate with regression grade (RG) in their study population with 21 LARC patients, although perfusion values were significantly higher in RG1 than RG2 at both pre- and post-cRT timepoints [65]. Several factors may contribute to the controversial findings, including small patient cohort size, differences in MR field strength and MR pulse sequence, and inherent random errors due to inconsistent timing between contrast injection and image acquisition. In two prospective semi-quantitative DCE studies with 75 and 88 LARC patients, Petrillo et al. showed the post-CRT standardized index of shape (SIS) of DCE was a superior predictor of treatment response, than IVIM and PET imaging, respectively [57, 58]. SIS is defined as the linear classifier maximizing area under ROC for change in maximum signal difference (MSD) and wash out slope (WOS). In the first study, ΔSIS achieved improved AUC of 0.86 and 0.82 than 18F-FDG PET-CT parameters for predicting responders (TRG1-2) and for predicting complete response (pCR) [57]. Similarly, in their second study, ΔSIS showed higher AUC than IVIM parameters in response prediction [58].

In quantitative DCE analysis, pharmacokinetic model fitting, usually the Tofts Model [66, 67], is applied to DCE concertation-time curve. From the Tofts Model, four main parameters can be extracted: K^{trans} (the transfer constant from vascular to extravascular extracellular space (EES)), v_e (volume fraction of EES in tissue), v_p (volume fraction of plasma in tissue), and k_{ep} (rate constant between the EES and the blood plasma). In a retrospective study with 40 LARC patients, Ciolina et al. showed pre-CRT K^{trans} was significantly higher for CR patients, suggesting K^{trans} could predict therapy response [59]. Additionally, Palmisano et al. prospectively analyzed quantitative pre-CRT DCE on 21 rectal cancer patients using a histogram-based approach and showed v_e skewness and kurtosis were significantly higher in non-GR than GR patients [60]. However, Yeo et al. applied histogram analysis on pre-CRT DCE MRI, and did not find a significant correlation between quantitative DCE parameters and TRG [68]. Zou et al. implemented texture analysis on pre- and

Table 2 Summary of key studies using DCE for rectal cancer CRT response prediction

Study	*n*	Study design	Imaging/analysis technique	Treatment response	Key results
Petrillo et al. (2018) [55]	158	Prospective	Pre-, post-CRT 1.5 T T2w MRI 1.5 T qualitative DCE MRI	Mandard TRG Responder (TRG1-2) Non-responder (TRG3-5)	Post-CRT qualitative DCE achieved superior CRT response prediction sensitivity (81% vs 52%), specificity (85% vs 78%), and accuracy (82% vs 62%) than T2w MRI
Ippolito et al. (2020) [56]	28	Prospective	Pre-, post-CRT 1.5 T semi-qualitative DCE MRI	Mandard TRG Responder (TRG1-2) Non-responder (TRG3-5)	Pre-CRT perfusion values were not significantly different between responders and non-responders Post-CRT perfusion parameters were significantly lower in responders than non-responders Responders showed significantly decreased perfusion values post-CRT
Petrillo et al. (2017) [57]	75	Prospective	Pre-, post-CRT 18F-FDG PET/CT 1.5 T semi-qualitative DCE MRI	Mandard TRG Responder (TRG1-2) Non-responders (TRG3-5) Complete responder (TRG1) Incomplete responder (TRG2-5)	Change in standardized-index-of-shape (SIS) derived from semi-quantitative DCE achieved an improved AUC of 0.86 and 0.82 than 18F-FDG PET-CT parameters for predicting CRT responders and complete responders
Petrillo et al. (2018) [58]	88	Prospective	Pre-, post-CRT 1.5 T quantitative IVIM MRI 1.5 T semi-qualitative DCE MRI	Mandard TRG Responder (TRG1-2) Non-responder (TRG3-5) Complete responder (TRG1) Incomplete responder (TRG2-5)	Change in standardized-index-of-shape (SIS) derived from semi-quantitative DCE achieved an improved AUC of 0.90 and 0.86 than IVIM MRI parameters for predicting CRT responders and complete responders
Ciolina et al. (2019) [59]	40	Retrospective	Pre-, post-CRT 3 T semi-qualitative DCE MRI 3 T quantitative DCE MRI	Mandard TRG Complete responder (TRG1) Incomplete response (TRG2-5)	Pre-CRT K^{trans} was significantly higher in complete responders than incomplete responders (0.66 ± 0.48 vs 0.53 ± 0.34)
Palmisano et al. (2018) [60]	21	Prospective	Pre-CRT 1.5 T quantitative DCE MRI (histogram-based)	Rodel TRG Poor responder (TRG0-2) Good responder (TRG3-4)	Pre-CRT v_e skewness and kurtosis were significantly higher in poor responders than good responders (4.886 ± 1.320 vs 1.809 ± 1.280; 36.402 ± 24.486 vs 6.268 ± 8.130)
Zou et al. (2019) [61]	83	Retrospective	Pre-, post-CRT 3 T quantitative DCE MRI (K^{trans} map texture analysis)	Mandard TRG Good responder (TRG1-2) Poor responder (TRG3-5) Complete responder (TRG1) Incomplete responder (TRG2-5)	Post-CRT tumor volume, mean K^{trans}, entropy, and correlation decreased, while energy significantly increased from pre-CRT for good and complete responders Change in correlation achieved an AUC of 0.895 for identify CR and GR patients
Napoletano et al. (2019) [62]	21	Retrospective	Pre, post-CRT 1.5 T T1w MRI 1.5 T T2w MRI 1.5 T qualitative DCE MRI 1.5 T qualitative DWI MRI	pSD — no response pPR — partial response pCR — complete response	Post-CRT, addition of qualitative DWI MRI to conventional MRI (T1w, T2w, DCE), improved diagnostic capacity of detecting response to 90.40%

Table 2 (continued)

Study	*n*	Study design	Imaging/analysis technique	Treatment response	Key results
Shi et al. (2019) [63]	51	Retrospective	Pre, mid-CRT 3.0 T T1w MRI 3.0 T T2w MRI 3.0 T DWI MRI 3.0 T DCE MRI Radiomics (ROI, GLCM texture, and histogram-based) Deep learning (convolutional neural network)	Complete responder (TRG0) Incomplete responder (TRG1-3) Good responder (TRG0-1) Non-good responder (TRG2-3)	The multi-modal radiomics model using pre- and mid-CRT T1w, T2w, DWI, and DCE MRI achieved an AUC of 0.86 and 0.93 for detecting complete and good responders The multi-modal deep learning model using pre- and mid-CRT T1w, T2w, DWI, and DCE MRI achieved an AUC of 0.83 and 0.74 for detecting complete and good responders
Li et al. (2020) [64]	118	Retrospective	Pre-CRT CT 3.0 T T2w MRI 3.0 T DWI MRI 3.0 T DCE MRI Radiomics (mRMR)	AJCC TRG Responder (TRG0-2) Non-responder (TRG3)	The multi-modal radiomics model using pre-CRT T2w, DWI, and DCE MRI achieved an AUC of 0.93 for detecting responders

post-CRT DCE MRI, and showed tumor volume, mean K^{trans}, entropy, and correlation decreased, while energy increased significantly for CR and GR patients. Moreover, change in correlation achieved an AUC of 0.895 for identifying CR and GR patients [61].

Semi-quantitative are less time-consuming and are easier to reproduce in comparison with quantitative [69]. Dijkhoff et al. showed a strong correlation between quantitative (K^{trans}, V_p) and semi-quantitative (peak-enhancement, wash-in) parameters in DCE for rectal cancer patients, before and after CRT [70]. As a result, semi-quantitative analysis can be used as a substitute for quantitative analysis.

Multi-parametric imaging has the potential to increase diagnostic and treatment response accuracy for LARC patients, utilizing key features or parameters of each technique. The key findings in multi-parametric studies for CRT treatment response are shown in Table 2. In a retrospectives study with 65 LARC patients, Gollub et al. showed visual inspection of post-CRT T2w and DWI achieved an AUC of 0.66, compared to digital rectal exams and endoscopy notes achieving an AUC of 0.69 to detect complete CRT responders. Furthermore, by combining the two techniques and adding visual DCE, observers were able to achieve an AUC of 0.72 [71]. In a similar study with 21 LARC patients, Napoletano et al. showed post-CRT T1w + T2w + visual DCE had a diagnostic capacity of 71.40% for detecting LARC CRT response. Then by adding qualitative DWI, the diagnostic capacity increased to 90.40% [62]. In contrast, study from Petrillo et al. showed linearly combining post-CRT semi-quantitative DCE and quantitative IVIM-DWI parameters did not improve response prediction performance compared to using standardized index of shape (SIS) from DCE or ΔADC alone. [58]

Through radiomics or deep learning methods, various multi-modal or multi-parametric values can be combined into high-dimensional quantitative features, revealing non-trivial disease markers. In a retrospective study with 51 LARC patients, Shi et al. used T1w, T2w, DWI, and DCE at pre- and mid-CRT treatment to generate a radiomics model using ROI-based, GLCM texture, and histogram parameters [63]. Additionally, a convolutional neural network (CNN) was designed using multi-parametric MRIs. The radiomics model achieved an AUC of 0.86 and 0.93, while the CNN achieved an AUC of 0.83 and 0.74 for predicting CR and GR. In a retrospective with 118 LARC patients, Li et al. developed a multi-modal radiomics to detect CRT response, combining pre-CRT CT and multi-parametric MRI [64]. Individually, the radiomics models for CT, T2w MRI, DCE, and ADC DWI achieved an AUC of 0.766, 0.859, 0.812, and 0.828. By combining all the techniques, the multi-modal radiomics model was able to achieve an AUC of 0.93.

Other Functional Imaging

In addition to diffusion and perfusion imaging, there are several other potential functional imaging biomarkers such as chemical exchange saturation transfer (CEST), blood oxygen level dependent (BOLD), or MR spectroscopy. In CEST imaging, a saturation pulse is applied, which is at the resonance frequency of a chemical species of interest and is capable of exchanging its ^{1}H protons with water. This saturation will be spontaneously transferred to water via chemical exchange and lead to a decrease in water signal that can be detected and used to reflect the concentration of the species of interest [72]. Nishie et al. acquired amide proton transfer (APT) imaging, an endogenous CEST technique, on 17 rectal cancer patients who underwent surgery after CRT. They found that the mean APT signal intensity of the low-response group was significantly higher than the intensity for the high-response group, whereas no difference was found based on ADC map [73].

BOLD imaging is based on the fact that deoxyhemoglobin is paramagnetic and has shorter T2 and T2*. Therefore, the image contrast reflects vascular oxygenation information that is potentially predictive of treatment response and patient prognosis. However, studies suggest that image contrast is more likely to reflect perfusion-related acute tissue hypoxia instead of diffusion-related chronic hypoxia caused by increased tumor expansion [74]. To date, there are not many studies investigating the correlation of BOLD-MRI with rectal treatment response.

MR spectroscopy measures spectral information within the imaging volume and provides important information for cancer chemical metabolism. Kim et al. acquired ^{1}H-MRS pre- and/or post-CRT on 134 patients [75]. A choline peak at 3.2 ppm was found on pre-CRT MRS, which can be used as a characteristic of rectal adenocarcinoma. For the 34 patients with both pre- and post-^{1}H-MRS, this choline peak disappeared on 97% of the patients, suggesting tumor response to CRT. Despite the promises, MR spectroscopy is mainly used in ex vivo setting than in clinical applications for rectal cancer due to limitations of low signal level, low spatial resolution, relatively long acquisition time, susceptibility to motion artifact, and non-ideal spectra quality due to local inhomogeneous [16]

Discussion and Future Directions

Functional MRI provides a promising tool for non-invasive treatment response assessment for LARC patients and has become an active research area. Despite promising preliminary results, applying functional MRI into clinical rectal cancer response assessment is still far from routine practice. One of the major issues is the lack of standardization. The majority of existing studies are performed retrospectively, which leads to large variations in terms of patient enrollment, imaging parameters, imaging time points, treatment prescription, endpoint definition, and analysis methods, etc. Because of this, a range of results were observed by different groups. For example, in terms of the best imaging time point of DWI for pCR prediction, there are studies supporting imaging at pre-CRT, mid-CRT, and post-CRT [29–35]. Therefore, it is crucial to standardize the workflow to comprehensively evaluate the usage of functional MRI for clinical rectal cancer response prediction.

Pham et al. proposed a detailed prospective study protocol for combined DWI, DCE, and PET/CT for therapeutic response prediction [76]. In this protocol, they clearly outlined patient selection criteria, imaging acquisition timeline, detailed imaging protocol, image analysis methods, and endpoint evaluation. This comprehensive study protocol could help to minimize the aforementioned variations, and may serve as an example protocol for multi-institutional collaboration.

Another limitation of many existing studies is the relatively small patient cohort size and lack of external validation. It is challenging to obtain large standardized medical data. However, the conclusion is vulnerable without the support of a sufficiently large patient number. Many studies only showed that the proposed imaging biomarker is able to successfully predict treatment response on their selected patient cohort. It is important to validate the model on a different group of patients, ideally external patients, to fully evaluate the prediction robustness. Therefore, cross-institution collaboration is a crucial step to collect a large number of patients, and ultimately enable the incorporation of functional MRI into the clinical care workflow.

In recent years, more studies have focused on multi-parametric imaging and quantitative analysis. Instead of using a signal contrast with limited information, combining different imaging contrasts, such as DWI, DCE, T2w, and T1w, provides a comprehensive view of tumor cellularity, vascularity, and morphological status post-CRT, which holds the promise of improved response prediction performance. Quantitative analysis such as radiomics and deep learning are now being widely used to uncover features that are not straightforward to human eyes. Although radiomic features and deep learning usually provide better prediction accuracy than conventional features, it is challenging to understand the mechanism of those features and models. Also, robustness and reproducibility of the selected features and models on other different cohorts warranted a thorough study.

Conclusions

Applying functional MRI to rectal cancer treatment response assessment is a promising area and has the potential of identifying patients with good and poor response for subsequent

individualized management. Current studies are still preliminary and focus mainly on the feasibility on a small selected patient cohort. To incorporate functional MRI into clinical workflow, standardization of the entire workflow and cross-institution collaboration are urgently needed. In the meantime, multi-parametric imaging and quantitative analysis are also future directions that could potentially improve the overall prediction accuracy.

Declarations

Human and Animal Rights and Informed Consent This article does not contain any studies with human or animal subjects performed by any of the authors.

Conflict of Interest Yu Gao, Jonathan Pham, Stephanie Yoon, and Minsong Cao each declare no potential conflicts of interest. Peng Hu has received consulting fees from ViewRay. Yingli Yang has received consulting fees and speaker honorarium from ViewRay.

References

Papers of particular interest, published recently, have been highlighted as: *Of importance **Of major importance

1. Gérard J-P, Conroy T, Bonnetain F, et al. Preoperative radiotherapy with or without concurrent fluorouracil and leucovorin in T3–4 rectal cancers: results of FFCD 9203. J Clin Oncol Off J Am Soc Clin Oncol. 2006;24(28):4620–5. https://doi.org/10.1200/JCO.2006.06.7629.
2. Sauer R, Becker H, Hohenberger W, et al. Preoperative versus postoperative chemoradiotherapy for rectal cancer. N Engl J Med. 2004;351(17):1731–40. https://doi.org/10.1056/NEJMoa040694.
3. Sauer R, Liersch T, Merkel S, et al. Preoperative versus postoperative chemoradiotherapy for locally advanced rectal cancer: results of the German CAO/ARO/AIO-94 randomized phase III trial after a median follow-up of 11 years. J Clin Oncol Off J Am Soc Clin Oncol. 2012;30(16):1926–33. https://doi.org/10.1200/JCO.2011.40.1836.
4. Ngan SY, Burmeister B, Fisher RJ, et al. Randomized trial of short course radiotherapy versus long-course chemoradiation comparing rates of local recurrence in patients with T3 rectal cancer: Trans-Tasman Radiation Oncology Group trial 01.04. J Clin Oncol Off J Am Soc Clin Oncol. 2012;30(31):3827–33. https://doi.org/10.1200/JCO.2012.42.9597.
5. Erlandsson J, Holm T, Pettersson D, et al. Optimal fractionation of preoperative radiotherapy and timing to surgery for rectal cancer (Stockholm III): a multicentre, randomised, non-blinded, phase 3, non-inferiority trial. Lancet Oncol. 2017;18(3):336–46. https://doi.org/10.1016/S1470-2045(17)30086-4.
6. Colorectal Cancer - Statistics. Cancer.Net. Published June 25, 2012. Accessed May 31, 2021. https://www.cancer.net/cancer-types/colorectal-cancer/statistics
7. Dworak O, Keilholz L, Hoffmann A. Pathological features of rectal cancer after preoperative radiochemotherapy. Int J Colorectal Dis. 1997;12(1):19–23.
8. Ryan R, Gibbons D, Hyland JMP, et al. Pathological response following long-course neoadjuvant chemoradiotherapy for locally advanced rectal cancer. Histopathology. 2005;47(2):141–6. https://doi.org/10.1111/j.1365-2559.2005.02176.x.
9. Mandard AM, Dalibard F, Mandard JC, et al. Pathologic assessment of tumor regression after preoperative chemoradiotherapy of esophageal carcinoma. Clinicopathologic correlations Cancer. 1994;73(11):2680–6. https://doi.org/10.1002/1097-0142(19940601)73:11%3c2680::aid-cncr2820731105%3e3.0.co;2-c.
10. Kapiteijn E, Marijnen CA, Nagtegaal ID, et al. Preoperative radiotherapy combined with total mesorectal excision for resectable rectal cancer. N Engl J Med. 2001;345(9):638–46. https://doi.org/10.1056/NEJMoa010580.
11. Janjan NA, Crane C, Feig BW, et al. Improved overall survival among responders to preoperative chemoradiation for locally advanced rectal cancer. Am J Clin Oncol. 2001;24(2):107–12.
12. Park IJ, You YN, Agarwal A, et al. Neoadjuvant treatment response as an early response indicator for patients with rectal cancer. J Clin Oncol Off J Am Soc Clin Oncol. 2012;30(15):1770–6. https://doi.org/10.1200/JCO.2011.39.7901.
13. Habr-Gama A, Perez RO, Nadalin W, et al. Operative versus nonoperative treatment for stage 0 distal rectal cancer following chemoradiation therapy: long-term results. Ann Surg. 2004;240(4):711–717; discussion 717–718.
14. Ellis CT, Samuel CA, Stitzenberg KB. National trends in nonoperative management of rectal adenocarcinoma. J Clin Oncol. Published online March 28, 2016:JCO642066. https://doi.org/10.1200/JCO.2015.64.2066
15. Yang TJ, Goodman KA. Predicting complete response: is there a role for non-operative management of rectal cancer? J Gastrointest Oncol. 2015;6(2):241–6. https://doi.org/10.3978/j.issn.2078-6891.2014.110.
16. Pham TT, Liney GP, Wong K, Barton MB. Functional MRI for quantitative treatment response prediction in locally advanced rectal cancer. Br J Radiol. 2017;90(1072):20151078. https://doi.org/10.1259/bjr.20151078.
17. Schurink NW, Lambregts DMJ, Beets-Tan RGH. Diffusion-weighted imaging in rectal cancer: current applications and future perspectives. Br J Radiol. 2019;92(1096):20180655. https://doi.org/10.1259/bjr.20180655.
18. Fusco R, Petrillo M, Granata V, et al. Magnetic resonance imaging evaluation in neoadjuvant therapy of locally advanced rectal cancer: a systematic review. Radiol Oncol. 2017;51(3):252–62. https://doi.org/10.1515/raon-2017-0032.
19. Park SH, Cho SH, Choi SH, et al. MRI assessment of complete response to preoperative chemoradiation therapy for rectal cancer: 2020 guide for practice from the Korean Society of Abdominal Radiology. Korean J Radiol. 2020;21(7):812–28. https://doi.org/10.3348/kjr.2020.0483.
20. Malayeri AA, El Khouli RH, Zaheer A, et al. Principles and applications of diffusion-weighted imaging in cancer detection, staging, and treatment follow-up. Radiogr Rev Publ Radiol Soc N Am Inc. 2011;31(6):1773–91. https://doi.org/10.1148/rg.316115515.
21. Moffat BA, Chenevert TL, Lawrence TS, et al. Functional diffusion map: a noninvasive MRI biomarker for early stratification of clinical brain tumor response. Proc Natl Acad Sci U S A. 2005;102(15):5524–9. https://doi.org/10.1073/pnas.0501532102.
22. Eisenhauer EA, Therasse P, Bogaerts J, et al. New response evaluation criteria in solid tumours: revised RECIST guideline (version 1.1). Eur J Cancer Oxf Engl 1990. 2009;45(2):228–247. https://doi.org/10.1016/j.ejca.2008.10.026
23. Lee MA, Cho SH, Seo AN, et al. Modified 3-point MRI-based tumor regression grade incorporating DWI for locally advanced rectal cancer. Am J Roentgenol. 2017;209(6):1247–55. https://doi.org/10.2214/AJR.16.17242.

24. Yoen H, Park HE, Kim SH, et al. Prognostic value of tumor regression grade on MR in rectal cancer: a large-scale, single-center experience. Korean J Radiol. 2020;21(9):1065–76. https://doi.org/10.3348/kjr.2019.0797.
25. Chandramohan A, Siddiqi UM, Mittal R, et al. Diffusion weighted imaging improves diagnostic ability of MRI for determining complete response to neoadjuvant therapy in locally advanced rectal cancer. Eur J Radiol Open. 2020;7. https://doi.org/10.1016/j.ejro.2020.100223
26. van Heeswijk MM, Lambregts DMJ, Palm WM, et al. DWI for assessment of rectal cancer nodes after chemoradiotherapy: is the absence of nodes at DWI proof of a negative nodal status? Am J Roentgenol. 2016;208(3):W79–84. https://doi.org/10.2214/AJR.16.17117.
27. Gollub MJ, Das JP, Bates DDB, et al. Rectal cancer with complete endoscopic response after neoadjuvant therapy: what is the meaning of a positive MRI? Eur Radiol. Published online January 15, 2021. https://doi.org/10.1007/s00330-020-07657-0
28. Shaverdian N, Yang Y, Hu P, et al. Feasibility evaluation of diffusion-weighted imaging using an integrated MRI-radiotherapy system for response assessment to neoadjuvant therapy in rectal cancer. Br J Radiol. 2017;90(1071):20160739. https://doi.org/10.1259/bjr.20160739.
29. De Felice F, Magnante AL, Musio D, et al. Diffusion-weighted magnetic resonance imaging in locally advanced rectal cancer treated with neoadjuvant chemoradiotherapy. Eur J Surg Oncol J Eur Soc Surg Oncol Br Assoc Surg Oncol. 2017;43(7):1324–9. https://doi.org/10.1016/j.ejso.2017.03.010.
30. Palmisano A, Di Chiara A, Esposito A, et al. MRI prediction of pathological response in locally advanced rectal cancer: when apparent diffusion coefficient radiomics meets conventional volumetry. Clin Radiol. 2020;75(10):798.e1-798.e11. https://doi.org/10.1016/j.crad.2020.06.023.
31. Yang L, Qiu M, Xia C, et al. Value of high-resolution DWI in combination with texture analysis for the evaluation of tumor response after preoperative chemoradiotherapy for locally advanced rectal cancer. AJR Am J Roentgenol. Published online March 12, 2019:1–8. https://doi.org/10.2214/AJR.18.20689
32. Bassaneze T, Gonçalves JE, Faria JF, Palma RT, Waisberg J. Quantitative aspects of diffusion-weighted magnetic resonance imaging in rectal cancer response to neoadjuvant therapy. Radiol Oncol. 2017;51(3):270–6. https://doi.org/10.1515/raon-2017-0025.
33. Tarallo N, Angeretti MG, Bracchi E, et al. Magnetic resonance imaging in locally advanced rectal cancer: quantitative evaluation of the complete response to neoadjuvant therapy. Pol J Radiol. 2018;83:e600–9. https://doi.org/10.5114/pjr.2018.81156.
34. Crimì F, Stramare R, Spolverato G, et al. T2-weighted, apparent diffusion coefficient and 18F-FDG PET histogram analysis of rectal cancer after preoperative chemoradiotherapy. Tech Coloproctol. 2021;25(5):569–77. https://doi.org/10.1007/s10151-021-02440-9.
35. Bulens P, Couwenberg A, Haustermans K, et al. Development and validation of an MRI-based model to predict response to chemoradiotherapy for rectal cancer. Radiother Oncol J Eur Soc Ther Radiol Oncol. 2018;126(3):437–42. https://doi.org/10.1016/j.radonc.2018.01.008.
36. Joye I, Debucquoy A, Deroose CM, et al. Quantitative imaging outperforms molecular markers when predicting response to chemoradiotherapy for rectal cancer. Radiother Oncol J Eur Soc Ther Radiol Oncol. 2017;124(1):104–9. https://doi.org/10.1016/j.radonc.2017.06.013.
37. Schurink NW, Min LA, Berbee M, et al. Value of combined multiparametric MRI and FDG-PET/CT to identify well-responding rectal cancer patients before the start of neoadjuvant chemoradiation. Eur Radiol. 2020;30(5):2945–54. https://doi.org/10.1007/s00330-019-06638-2.
38.•• Tang Z, Zhang X-Y, Liu Z, et al. Quantitative analysis of diffusion weighted imaging to predict pathological good response to neoadjuvant chemoradiation for locally advanced rectal cancer. Radiother Oncol J Eur Soc Ther Radiol Oncol. 2019;132:100–8. https://doi.org/10.1016/j.radonc.2018.11.007. **A large patient cohort study (152 training and 70 validation) investigating the usage of radiomics and clinical characteristics for LARC down-staging prediction.**
39. Bulens P, Couwenberg A, Intven M, et al. Predicting the tumor response to chemoradiotherapy for rectal cancer: model development and external validation using MRI radiomics. Radiother Oncol J Eur Soc Ther Radiol Oncol. 2020;142:246–52. https://doi.org/10.1016/j.radonc.2019.07.033.
40. Chen F, Ma X, Li S, et al. MRI-based radiomics of rectal cancer: assessment of the local recurrence at the site of anastomosis. Acad Radiol. Published online November 5, 2020. https://doi.org/10.1016/j.acra.2020.09.024
41. Wan L, Peng W, Zou S, et al. MRI-based delta-radiomics are predictive of pathological complete response after neoadjuvant chemoradiotherapy in locally advanced rectal cancer. Acad Radiol. Published online November 11, 2020. https://doi.org/10.1016/j.acra.2020.10.026
42. van Griethuysen JJM, Lambregts DMJ, Trebeschi S, et al. Radiomics performs comparable to morphologic assessment by expert radiologists for prediction of response to neoadjuvant chemoradiotherapy on baseline staging MRI in rectal cancer. Abdom Radiol. 2020;45(3):632–43. https://doi.org/10.1007/s00261-019-02321-8.
43. Nardone V, Reginelli A, Scala F, et al. Magnetic-resonance-imaging texture analysis predicts early progression in rectal cancer patients undergoing neoadjuvant chemoradiation. Gastroenterol Res Pract. 2019;2019:e8505798. https://doi.org/10.1155/2019/8505798.
44. Fu J, Zhong X, Li N, et al. Deep learning-based radiomic features for improving neoadjuvant chemoradiation response prediction in locally advanced rectal cancer. Phys Med Biol. 2020;65(7):075001. https://doi.org/10.1088/1361-6560/ab7970.
45. Gillies RJ, Kinahan PE, Hricak H. Radiomics: images are more than pictures, they are data. Radiology. 2015;278(2):563–77. https://doi.org/10.1148/radiol.2015151169.
46. Le Bihan D, Breton E, Lallemand D, Aubin ML, Vignaud J, Laval-Jeantet M. Separation of diffusion and perfusion in intravoxel incoherent motion MR imaging. Radiology. 1988;168(2):497–505. https://doi.org/10.1148/radiology.168.2.3393671.
47. Lu W, Jing H, Ju-Mei Z, et al. Intravoxel incoherent motion diffusion-weighted imaging for discriminating the pathological response to neoadjuvant chemoradiotherapy in locally advanced rectal cancer. Sci Rep. 2017;7(1):8496. https://doi.org/10.1038/s41598-017-09227-9.
48.• Xu Q, Xu Y, Sun H, et al. Quantitative intravoxel incoherent motion parameters derived from whole-tumor volume for assessing pathological complete response to neoadjuvant chemotherapy in locally advanced rectal cancer. J Magn Reson Imaging JMRI. 2018;48(1):248–58. https://doi.org/10.1002/jmri.25931. **A prospective study showing IVIM-derived parameters are superior to ADC-based parameter in pCR prediction.**
49. Hu H, Jiang H, Wang S, Jiang H, Zhao S, Pan W. 3.0 T MRI IVIM-DWI for predicting the efficacy of neoadjuvant chemoradiation for locally advanced rectal cancer. Abdom Radiol N Y. 2021;46(1):134–43. https://doi.org/10.1007/s00261-020-02594-4.
50. Zhu H-B, Zhang X-Y, Zhou X-H, et al. Assessment of pathological complete response to preoperative chemoradiotherapy by means of multiple mathematical models of diffusion-weighted MRI in locally advanced rectal cancer: a

prospective single-center study. J Magn Reson Imaging JMRI. 2017;46(1):175–83. https://doi.org/10.1002/jmri.25567.
51. Liang C-Y, Chen M-D, Zhao X-X, Yan C-G, Mei Y-J, Xu Y-K. Multiple mathematical models of diffusion-weighted magnetic resonance imaging combined with prognostic factors for assessing the response to neoadjuvant chemotherapy and radiation therapy in locally advanced rectal cancer. Eur J Radiol. 2019;110:249–55. https://doi.org/10.1016/j.ejrad.2018.12.005.
52. Liu S, Wen L, Hou J, et al. Predicting the pathological response to chemoradiotherapy of non-mucinous rectal cancer using pretreatment texture features based on intravoxel incoherent motion diffusion-weighted imaging. Abdom Radiol N Y. 2019;44(8):2689–98. https://doi.org/10.1007/s00261-019-02032-0.
53. Jensen JH, Helpern JA. MRI quantification of non-Gaussian water diffusion by kurtosis analysis. NMR Biomed. 2010;23(7):698–710. https://doi.org/10.1002/nbm.1518.
54. Hu F, Tang W, Sun Y, et al. The value of diffusion kurtosis imaging in assessing pathological complete response to neoadjuvant chemoradiation therapy in rectal cancer a comparison with conventional diffusion-weighted imaging. Oncotarget. 2017;8(43):75597–606. https://doi.org/10.18632/oncotarget.17491.
55. Petrillo A, Fusco R, Petrillo M, et al. DCE-MRI time–intensity curve visual inspection to assess pathological response after neoadjuvant therapy in locally advanced rectal cancer. Jpn J Radiol. 2018;36(10):611–21. https://doi.org/10.1007/s11604-018-0760-1.
56.•• Ippolito D, Drago SG, Pecorelli A, et al. Role of dynamic perfusion magnetic resonance imaging in patients with local advanced rectal cancer. World J Gastroenterol. 2020;26(20):2657–68. https://doi.org/10.3748/WJG.V26.I20.2657. **Prospective semi-quantitative DCE study showing post-CRT responders with significantly lower perfusion than non-responders.**
57. Petrillo A, Fusco R, Petrillo M, et al. Standardized Index of Shape (DCE-MRI) and Standardized Uptake Value (PET/CT) two quantitative approaches to discriminate chemo-radiotherapy locally advanced rectal cancer responders under a functional profile. Oncotarget. 2017;8(5):8143–53. https://doi.org/10.18632/oncotarget.14106.
58. Petrillo A, Fusco R, Granata V, et al. Assessing response to neoadjuvant therapy in locally advanced rectal cancer using Intravoxel Incoherent Motion modelling by DWI data and Standardized Index of Shape from DCE-MRI. Ther Adv Med Oncol. 2018;10. https://doi.org/10.1177/1758835918809875
59. Ciolina M, Caruso D, De Santis D, et al. Dynamic contrast-enhanced magnetic resonance imaging in locally advanced rectal cancer: role of perfusion parameters in the assessment of response to treatment. Radiol Med (Torino). 2019;124(5):331–8. https://doi.org/10.1007/s11547-018-0978-0.
60. Palmisano A, Esposito A, Rancoita PMV, et al. Could perfusion heterogeneity at dynamic contrast-enhanced MRI be used to predict rectal cancer sensitivity to chemoradiotherapy? Clin Radiol. 2018;73(10):911.e1-911.e7. https://doi.org/10.1016/j.crad.2018.06.007.
61. Zou HH, Yu J, Wei Y, Wu JF, Xu Q. Response to neoadjuvant chemoradiotherapy for locally advanced rectum cancer: texture analysis of dynamic contrast-enhanced MRI. J Magn Reson Imaging. 2019;49(3):885–93. https://doi.org/10.1002/jmri.26254.
62. Napoletano M, Mazzucca D, Prosperi E, et al. Locally advanced rectal cancer: qualitative and quantitative evaluation of diffusion-weighted magnetic resonance imaging in restaging after neoadjuvant chemoradiotherapy. Abdom Radiol. 2019;44(11):3664–73. https://doi.org/10.1007/s00261-019-02012-4.
63. Shi L, Zhang Y, Nie K, et al. Machine learning for prediction of chemoradiation therapy response in rectal cancer using pre-treatment and mid-radiation multi-parametric MRI. Magn Reson Imaging. 2019;61:33–40. https://doi.org/10.1016/j.mri.2019.05.003.
64.•• Li Z-Y, Wang X-D, Li M, et al. Multi-modal radiomics model to predict treatment response to neoadjuvant chemotherapy for locally advanced rectal cancer. World J Gastroenterol. 2020;26(19):2388–402. https://doi.org/10.3748/wjg.v26.i19.2388. **Multi-modality/parametric radiomic model using CT, T2w, DCE, and DWI MRI showing high accuracy of predicting treatment response, prior to CRT.**
65. Attenberger UI, Ong MM, Rathmann N, et al. MMRI at 3.0 T as an evaluation tool of therapeutic response to neoadjuvant CRT in patients with advanced-stage rectal cancer. Anticancer Res. 2017;37(1):215–22. https://doi.org/10.21873/anticanres.11309.
66. Tofts PS. Modeling tracer kinetics in dynamic Gd-DTPA MR imaging. J Magn Reson Imaging JMRI. 1997;7(1):91–101. https://doi.org/10.1002/jmri.1880070113.
67. Tofts PS, Brix G, Buckley DL, et al. Estimating kinetic parameters from dynamic contrast-enhanced T(1)-weighted MRI of a diffusable tracer: standardized quantities and symbols. J Magn Reson Imaging JMRI. 1999;10(3):223–32. https://doi.org/10.1002/(sici)1522-2586(199909)10:3%3c223::aid-jmri2%3e3.0.co;2-s.
68. Yeo DM, Oh SN, Choi MH, Lee SH, Lee MA, Jung SE. Histogram analysis of perfusion parameters from dynamic contrast-enhanced MR imaging with tumor characteristics and therapeutic response in locally advanced rectal cancer. BioMed Res Int. 2018;2018. https://doi.org/10.1155/2018/3724393
69. Dijkhoff RAP, Beets-Tan RGH, Lambregts DMJ, Beets GL, Maas M. Value of DCE-MRI for staging and response evaluation in rectal cancer: a systematic review. Eur J Radiol. 2017;95:155–68. https://doi.org/10.1016/j.ejrad.2017.08.009.
70. Dijkhoff RAP, Maas M, Martens MH, et al. Correlation between quantitative and semiquantitative parameters in DCE-MRI with a blood pool agent in rectal cancer: can semiquantitative parameters be used as a surrogate for quantitative parameters? Abdom Radiol. 2017;42(5):1342–9. https://doi.org/10.1007/s00261-016-1024-0.
71. Gollub MJ, Blazic I, Felder S, et al. Value of adding dynamic contrast-enhanced MRI visual assessment to conventional MRI and clinical assessment in the diagnosis of complete tumour response to chemoradiotherapy for rectal cancer. Eur Radiol. 2019;29(3):1104–13. https://doi.org/10.1007/s00330-018-5719-1.
72. Ward KM, Aletras AH, Balaban RS. 2000 A new class of contrast agents for MRI based on proton chemical exchange dependent saturation transfer (CEST). J Magn Reson San Diego Calif. 1997;143(1):79–87. https://doi.org/10.1006/jmre.1999.1956.
73. Nishie A, Takayama Y, Asayama Y, et al. Amide proton transfer imaging can predict tumor grade in rectal cancer. Magn Reson Imaging. 2018;51:96–103. https://doi.org/10.1016/j.mri.2018.04.017.
74. García-Figueiras R, Baleato-González S, Padhani AR, et al. Advanced imaging of colorectal cancer: from anatomy to molecular imaging. Insights Imaging. 2016;7(3):285–309. https://doi.org/10.1007/s13244-016-0465-x.
75. Kim MJ, Lee SJ, Lee JH, et al. Detection of rectal cancer and response to concurrent chemoradiotherapy by proton magnetic resonance spectroscopy. Magn Reson Imaging. 2012;30(6):848–53. https://doi.org/10.1016/j.mri.2012.02.013.
76.•• Pham TT, Liney G, Wong K, et al. Study protocol: multi-parametric magnetic resonance imaging for therapeutic response prediction in rectal cancer. BMC Cancer. 2017;17(1):465. https://doi.org/10.1186/s12885-017-3449-4. **This paper provided an example study protocol, such as patient selection, imaging acquisition, image analysis method, and endpoint evaluation, for using functional MR for rectal cancer treatment response.**